

Stabilization of a Majorana Zero Mode through Quantum Frustration

Gu Zhang^{1,2} and Harold U. Baranger^{1,*}

¹*Department of Physics, Duke University, P.O. Box 90305, Durham, North Carolina 27708, USA*

²*Institute for Quantum Materials and Technologies, Karlsruhe Institute of Technology, 76021 Karlsruhe, Germany*[†]

(Dated: May 28, 2020)

We analyze a system in which a topological Majorana zero mode (tMZM) combines with a Majorana produced by quantum frustration (fMZM) to produce a novel ground state. The system that we study combines two parts, a grounded topological superconducting wire that hosts two tMZMs at its ends, and an on-resonant quantum dot connected to two dissipative leads. The quantum dot with dissipative leads creates an effective two-channel Kondo (2CK) state in which quantum frustration yields an isolated fMZM at the dot. We find that coupling the dot to one end of the topological wire stabilizes the tMZM at the other end. Three routes are used to obtain these results: (i) calculation of the conductance through an auxiliary detector quantum dot, (ii) renormalization group (RG) arguments and the g -theorem, and (iii) a fully non-equilibrium calculation of the $I(V)$ curve and shot noise $S(V)$ through the detector dot. In addition to providing a route to achieving an unpaired Majorana zero mode, this scheme provides a clear signature of the presence of the 2CK frustration-induced Majorana.

I. INTRODUCTION

Electron states with topological character and quantum frustration from competing interactions are two major themes in current condensed matter physics. In both contexts, fractionalized degrees of freedom on the boundary of a system occur. Perhaps the best known example is the possibility of Majorana zero modes (MZMs) at the ends of a one-dimensional (1D) system. MZMs are exotic self-conjugate edge states that can occur through either topology [1–4] or fine-tuning of competing interactions [5–9]. Here we study the interplay between a topological Majorana zero mode (tMZM) and frustration-induced Majorana (fMZM) in a nanoscale system of quantum dots and wires. We show that a fMZM can stabilize a tMZM.

Quantum frustration typically produces states of matter that are delicately balanced between competing options and which then show fractionalization [10]. Quantum impurity models—an interacting quantum system coupled to leads—provide several canonical examples. (Note that quantum impurity models are effectively 1D since the impurity couples to a limited set of states in the leads [11].) The two channel Kondo (2CK) model, for instance, has been extensively studied [5, 6, 9, 12, 13]: an impurity spin is equally coupled to two metallic leads. It would be natural for the impurity spin to form a singlet with each lead, but it cannot because of entanglement exhaustion. This frustration in screening the impurity leads to a non-Fermi-liquid ground state in which there is a degeneracy of $\sqrt{2}$ at the impurity. This signals fractionalization and the existence of an unpaired fMZM [14]. It has also been discussed in the two impurity Kondo model [8, 15] and the dissipative resonant level model [16, 17]. Experimentally, several groups have investigated in detail nanoscale systems with an unpaired fMZM of this type [16, 18–22]—to date, the fine tuning required appears to be easier to achieve than the creation of a topological state.

Topological MZMs, in addition to their inherent interest, have attracted attention because their non-Abelian statistics provide a possible route toward fault tolerant quantum computation [1, 23]. To construct and observe such MZMs, researchers have proposed multiple systems [3, 24–27]. One particularly promising 1D system consists of a semiconducting nanowire made of a material that has strong spin-orbit coupling which is placed in proximity to a s -wave superconductor and in a magnetic field [3]. In this system, signatures of tMZM through measurement of the conductance have been intensively pursued [3].

In contrast to the free elementary particle predicted by Majorana, the effective tMZMs in condensed matter always appear in pairs in finite size systems [1, 3]. Unfortunately, tMZMs lose many of their interesting properties when they hybridize with their partners. The inter-MZM coupling decays as $\propto \exp(-L/\xi)$ [1, 3], with L the distance and ξ the superconducting correlation length in the nanowire. Experimentally, this hybridization can not generally be ignored [3]. Consequently, to see the full effect of a tMZM, a method to stabilize the tMZM against inter-MZM coupling is desirable.

In this paper, we stabilize a tMZM against hybridization with its partner by coupling that partner to an unpaired Majorana fermion of a dissipative quantum dot. Through this stabilization, the frustration-induced fMZM of the $R = R_Q \equiv h/e^2$ dissipative resonant level model can be experimentally detected.

We emphasize that “stabilization” here is understood in the renormalization group (RG) sense. In the absence of stabilization, we show that a finite inter-tMZM coupling, no matter how small, is RG *relevant*: it effectively increases with decreasing temperature and thus drastically changes the system ground state. In contrast, when the dissipation-induced fMZM is present, the inter-tMZM coupling is *irrelevant* and vanishes at zero temperature, regardless of its bare value. Because of this RG aspect, the stabilization studied here is qualitatively different from other proposals where the bare inter-tMZM coupling can be reduced to zero through fine tuning. See Refs. [2, 28–31] for examples of fine tuning by increasing the nanowire size, coupling the nanowire to a quantum dot, or

* baranger@phy.duke.edu

† gu.zhang@kit.edu

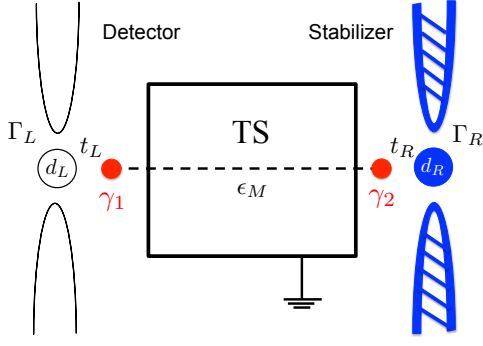


FIG. 1. The structure of the system. Two tMZMs γ_1 and γ_2 are realized at two ends of a nanowire on top of a grounded topological superconductor (TS). We calculate the conductance through the left quantum dot to detect the existence of the tMZM γ_1 . The right quantum dot, through which transport is dissipative (blue), couples to γ_2 and thereby stabilizes γ_1 as an isolated tMZM.

through electronic interactions.

The rest of the paper is organized as follows. We begin with the introduction of our model in Sec. II. After that, Sec. III contains a brief review of the dissipative resonant level model and its frustration-induced Majorana fermion. With those ingredients, we calculate in Sec. IV the conductance through the detector quantum dot (the left side of Fig. 1) that couples to one of the tMZM. These results allow us to conclude that the fMZM of a dissipative resonant level model stabilizes the tMZM by coupling to its partner, thus leaving a single unpaired tMZM. We further interpret the result with the g-theorem of boundary conformal field theory in Sec. IV D, where we stress the importance of the dissipation-induced fMZM in the process of stabilization. To gain further information and support for our view, we find the non-equilibrium conductance and shot noise through the detector quantum dot with full counting statistics methods in Sec. V. Our results indicate that there is an abrupt transition of the ground state when the fMZM joins the system. This transition can be clearly observed through conductance, shot noise, as well as the Fano factor of the detecting resonant level. Finally, we summarize our paper in Sec. VI.

II. THE SYSTEM

The system we consider consists of three major parts: (i) a superconducting nanowire that hosts two tMZMs, (ii) a resonant level that detects the presence of a tMZM by its conductance, and (iii) a dissipative resonant level, formed in a quantum dot, which introduces a fMZM that stabilizes the signature of the tMZM.

We consider the superconducting nanowire as a bare bones system, shown in Fig. 1, that has a pair of tMZM, γ_1 and γ_2 (red dots), at its ends. The coupling between these two tMZMs is $\epsilon_M \neq 0$ and hence the Hamiltonian of the system is

$$H_{\text{sys.}} = i\epsilon_M \gamma_1 \gamma_2. \quad (1)$$

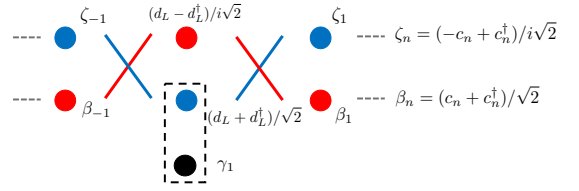


FIG. 2. A resonant level (with operators c_n and c_n^\dagger for the n th site in the leads) couples to a tMZM γ_1 . When fine-tuning, the resonant level system can be considered as two independent Majorana chains [32] (indicated by red and blue colors, respectively). The tMZM γ_1 and $(d_L + d_L^\dagger)/\sqrt{2}$ form into a singlet (indicated by the black dashed box), thus breaking one of the Majorana channels (the blue one). The conductance becomes $e^2/2h$, totally from the red Majorana channel.

The goal is to have effectively $\epsilon_M = 0$ so that even at zero temperature the topological feature of γ_1 is evident.

In order to assess directly whether γ_1 is indeed an independent tMZM, we incorporate a detector explicitly. As the presence of a tMZM affects many physical properties, different types of detectors could be used. We choose to consider the conductance through a spinless quantum dot modeled as a resonant level [32], pictured on the left of Fig. 1. As there are no interactions here, the Hamiltonian of the detector is simply

$$H_{\text{detect.}} = \epsilon_L d_L^\dagger d_L + \sum_{k,\alpha} \epsilon_k c_{kL\alpha}^\dagger c_{kL\alpha} + V_L \sum_{k,\alpha} \left(c_{kL\alpha}^\dagger d_L + d_L^\dagger c_{kL\alpha} \right), \quad (2)$$

where ϵ_L is the dot energy level, $c_{kL\alpha}$ is for electrons in the $\alpha = S$ (source) or D (drain) lead, and V_L is the dot-lead coupling. We assume that the dot is tuned to resonance, $\epsilon_L = 0$, and symmetrically coupled to the leads.

The tMZM γ_1 is tunnel coupled to a combination of d_L and d_L^\dagger . Because $\epsilon_L = 0$, all such combinations are equivalent and so we take

$$H_{\text{sys.-det.}} = it_L \frac{d_L^\dagger + d_L}{\sqrt{2}} \gamma_1. \quad (3)$$

The (zero-temperature) conductance through the left dot, denoted G_L , for $H = H_{\text{sys.}} + H_{\text{detect.}} + H_{\text{sys.-det.}}$ has been studied previously [32]. There is a clear signature of the coupling to the topological Majorana: while $G_L = e^2/h$ on resonance for a classic resonant level ($t_L = 0$), in the presence of the tMZM one obtains half that value, $G_L = e^2/2h$. Intuitively, the tMZM hybridizes with part of the resonant level and so blocks the conductance of a “half chain”, as illustrated in Fig. 2 [32]. Thus, we shall use $G_L = e^2/2h$ as the sign that a tMZM is present.

However, for any non-zero ϵ_M , the conductance reverts to the topologically trivial $G_L = e^2/h$ at low temperature, $T \ll \epsilon_M$. Indeed, ϵ_M is RG relevant, as shown below, and so grows large at low temperature regardless of its bare value (i.e., the value determined by the experimental system). The resulting extreme sensitivity to the value of ϵ_M makes observation of the tMZM especially difficult.

In order to stabilize γ_1 , one natural idea is to couple its partner γ_2 to an isolated Majorana fermion, thereby removing it from potentially hybridizing with γ_1 . Fortunately, such an isolated Majorana fermion is known to exist in the 2CK quantum impurity model. Specifically, the frustration between the two channels leaves an effective fMZM $(d + d^\dagger)/\sqrt{2}$ untouched, where $d \equiv iS_x - S_y$ is the effective fermionic operator and S_σ are the Pauli matrices of the impurity spin [6, 9, 33]. However, this effective fMZM is fundamentally a *spin* operator and so will not naturally couple with the *spatial* degree of freedom γ_2 .

To solve this problem, we propose to generate an isolated fMZM with a dissipative quantum dot [16, 19]. The corresponding resonant level model with ohmic impedance $R = R_Q$ [16, 17] is known to be equivalent to the 2CK model as well as the Luttinger liquid resonant level model with Luttinger liquid interaction $g = 1/2$. The quantum dot forming the resonant level hosts a real [34] decoupled Majorana fermion [16, 17]. Since this fMZM involves a *spatial* degree of freedom, we can model its coupling to γ_2 with the standard inter-Majorana coupling.

III. QUANTUM FRUSTRATION FROM DISSIPATION: THE DISSIPATIVE RESONANT LEVEL MODEL

We begin by sketching the needed elements of the theory of the dissipative resonant level model [16, 17, 19, 35], emphasizing the formation of its dissipation-induced fMZM. The dissipative resonant level model describes a quantum dot that couples to two dissipative spin-polarized leads. It is defined by the Hamiltonian [35–37]

$$\begin{aligned} H_{\text{dissip.}} &= H_{\text{dot}} + H_{\text{lead}} + H_{\text{T}} \\ &= \epsilon_R d^\dagger d + \sum_{k,\alpha} \epsilon_k c_{k\alpha}^\dagger c_{k\alpha} \\ &\quad + \sum_{k,\alpha} V_\alpha \left(e^{-i\phi_\alpha} c_{k\alpha}^\dagger d + e^{+i\phi_\alpha} d^\dagger c_{k\alpha} \right), \end{aligned} \quad (4)$$

where $\alpha = S, D$ for the source and drain, respectively. The notation parallels that for the detector: ϵ_R is the dot energy level, $c_{k\alpha}^\dagger$ creates an electron in the lead labeled α , and lead α couples to the dot with strength V_α . The key aspect of the model is the coupling to dissipation in the tunneling term [third line of Eq. (4)].

In modeling the dissipation, we follow a standard approach [36–38]. The phase fluctuation operator ϕ_α is conjugate to the charge fluctuation operator for the capacitor between the dot and lead α . Thus, the operator $e^{\pm i\phi_\alpha}$ in Eq. (4) accounts for the change in charge upon tunneling. The current and voltage fluctuations caused by the electrons tunneling on and off the dot excite the ohmic environment of the leads. This environment is modeled as a bath of harmonic oscillators [36–39]. Because it is the charge moving across the dot that excites the environment, the difference $\varphi \equiv \phi_S - \phi_D$ couples to the harmonic oscillators. The bath causes the correlation function of these fluctuations to be

$$\langle e^{-i\varphi(t)} e^{i\varphi(0)} \rangle \propto (1/t)^{2r} \quad (5)$$

where the exponent r is related to the resistance of the environment by $r \equiv Re^2/h \equiv R/R_Q$. With this correlation function, the conductance and scaling behavior can be found.

Interactions are thus introduced by the dissipation [i.e. the third line of Eq. (4) is *not* quadratic]—theoretically, we are faced with an *interacting quantum impurity* model. It is then natural to proceed with a bosonization treatment followed by renormalization (RG) [9, 16, 17, 40–44].

Following the standard technique [9, 35], we unfold each lead into an infinite chiral fermion channel and then apply chiral bosonization,

$$c_\alpha(x) = \frac{F_\alpha}{\sqrt{2\pi a}} e^{i\phi_\alpha(x) + ik_F x}, \quad (6)$$

where F_α is the Klein factor $\{F_\alpha, F_{\alpha'}\} = 2\delta_{\alpha,\alpha'}$ that preserves the fermionic commutation relations, and a is the lattice constant. The bosonic field operator ϕ_α , representing the collective modes of the corresponding chiral channel [9], has the standard commutation relation

$$[\partial_x \phi_\alpha(x), \phi_{\alpha'}(x')] = i\delta_{\alpha,\alpha'} \pi \delta(x - x'). \quad (7)$$

We further define fields in the common (ϕ_c) and difference (ϕ_f) sectors through the rotation

$$\phi_f = \frac{\phi_S - \phi_D}{\sqrt{2}}, \quad \phi_c = \frac{\phi_S + \phi_D}{\sqrt{2}}. \quad (8)$$

The fields ϕ_c and ϕ_f reflect the dot occupation number and the electron number difference between two leads, respectively.

Substituting these bosonization expressions into the Hamiltonian (4), one finds that the bosonic field ϕ_f and dissipative phase φ appear in the same way in the tunneling term. As they both have power-law correlation functions [Eq. (5) and [9]], we therefore combine them with the transformation

$$\begin{aligned} \phi'_f &\equiv \frac{1}{\sqrt{1+r}} \left(\phi_f + \frac{1}{\sqrt{2}} \varphi \right) \\ \varphi' &\equiv \frac{1}{\sqrt{1+r}} \left(\sqrt{r} \phi_f + \frac{1}{\sqrt{2r}} \varphi \right), \end{aligned} \quad (9)$$

through which the tunneling Hamiltonian becomes [17, 35]

$$H_{\text{T}} = \sum_{\alpha \in \{S,D\}} \frac{V_\alpha}{\sqrt{2\pi a}} \left(e^{-i\frac{1}{\sqrt{2}}\phi_c} e^{-i\alpha\sqrt{\frac{1+r}{2}}\phi'_f} F_\alpha d + \text{h.c.} \right), \quad (10)$$

where $\alpha = \pm 1$ for source and drain, respectively.

Eq. (10) effectively mimics the tunneling Hamiltonian of a Luttinger liquid in which the interaction in the common (c) and difference (f) sectors is different. (For related work on links between the physics of Luttinger liquids and dissipative tunneling see, e.g., Refs. [45–50].) Following the well-established RG technique for Luttinger liquids [9, 40, 43], we

obtain RG equations when $\epsilon_R = 0$ [35, 43]:

$$\begin{aligned} \frac{dV_S}{d \ln \tau_c} &= \left[1 - \left(\frac{1+r}{4} + \frac{K_1}{4} + \frac{K_2}{2} \right) \right] V_S, \\ \frac{dV_D}{d \ln \tau_c} &= \left[1 - \left(\frac{1+r}{4} + \frac{K_1}{4} - \frac{K_2}{2} \right) \right] V_D, \\ \frac{dK_1}{d \ln \tau_c} &= -4\tau_c^2 \left[(V_S^2 + V_D^2) K_1 + (V_S^2 - V_D^2) K_2 \right], \\ \frac{dK_2}{d \ln \tau_c} &= -2\tau_c^2 \left[(V_S^2 + V_D^2) K_2 + (V_S^2 - V_D^2) \right], \end{aligned} \quad (11)$$

where τ_c is the energy cutoff that decreases gradually with the decreasing temperature, and K_1, K_2 are the fugacity parameters that incorporate the symmetric and anti-symmetric parts of the dot- ϕ_c interaction during the RG flow. Initially, $K_1 = 1$ and $K_2 = 0$. Importantly, for finite asymmetry $V_S - V_D$, $|K_2|$ increases, which in turn leads to increased asymmetry upon RG flow. Generically, the flow thus ends at a ground state in which the quantum dot is completely hybridized with either the source or the drain (and cut from the other), depending on whether V_S or V_D is initially larger. The transition between these two candidate ground states, known as a boundary quantum phase transition, has been experimentally realized [16, 19].

Non-trivial behavior appears at the quantum critical point $V_S = V_D$: *frustration* between hybridization with the source versus the drain prevents the quantum dot from being fully hybridized. In fact, a finite residual entropy $\ln\sqrt{1+r}$ remains at zero temperature [7]. This residual entropy mimics that of the 2CK problem at the intermediate fixed point [16, 17, 44, 51], where a spin Majorana becomes isolated due to overscreening. Specially, when $R = R_Q$ (i.e. $r = 1$), the residual entropy at the fine-tuned quantum critical point becomes $\ln\sqrt{2}$, which coincides with that of a Majorana fermion. *This Majorana is the fMZM we use in this paper to stabilize the tMZM.*

For $R = R_Q$ the model has been thoroughly investigated through bosonization and refermionization [16, 17, 51], following that for the 2CK model [6, 33, 52] or a $g = 1/2$ Luttinger liquid resonant level model [9]. Following their example, we apply the unitary transformation

$$U = e^{i(d^\dagger d - \frac{1}{2})\phi_c(0)/\sqrt{2}}, \quad (12)$$

to remove the common field ϕ_c from the tunneling term. However, this unitary transformation introduces two minor side effects. First, the impurity operator is now dressed with the common field $\phi_c(0)$,

$$d \rightarrow d e^{iK_1 \frac{1}{\sqrt{2}} \phi_c(0)}, \quad (13)$$

with $K_1 = 1$ initially, i.e. before the RG flow of Eq. (11). Second, the unitary transformation introduces a quartic interaction [17, 35],

$$H_{\text{extra}} = -\frac{v}{2\sqrt{2}} \left(d^\dagger d - \frac{1}{2} \right) \partial_x \phi_c(x) \Big|_{x=0} \quad (14)$$

where v is the Fermi velocity, that couples ϕ_c to the impurity occupation number.

Strictly, the phase factor $\exp[i\phi_c(0)/\sqrt{2}]$ that attaches to d as well as the interaction Eq. (14) are quite important at high temperatures [17]. However, K_1 decreases according to the RG equations (11) [43], so that at low temperature $d \exp[iK_1\phi_c(0)/\sqrt{2}]$ and the bare operator d become indistinguishable. With regard to the induced density-density interaction (14), it has scaling dimension 3/2 (see, for instance, [53] or [54] where similar terms have been encountered) and is thus RG irrelevant. Consequently, as we are only interested in the low temperature physics near the ground state, *both* the phase attached to impurity operators and the quartic interaction can be safely neglected.

Finally, we define a Majorana representation for the degree of freedom represented by d : $\chi_1 \equiv (d^\dagger + d)/\sqrt{2}$ and $\chi_2 \equiv i(d^\dagger - d)/\sqrt{2}$. Because of the unitary transformation mentioned in the last paragraph, this is no longer simply the dot level but rather a nonlinear mixture of the dot and the density in the two leads near the dot. Both resulting MZMs are highly localized near the quantum dot.

For the specific case $r = 1$, the dependence on the difference field ϕ'_f in (10) can be expressed as a fermionic operator $\psi_f \equiv e^{i\phi'_f}/\sqrt{2\pi a}$ (using the Klein factor from the original bosonization). The result of these manipulations is an effective Majorana Hamiltonian for the right-hand dot and leads:

$$\begin{aligned} H_{\text{dissip.}} &= \sum_k \epsilon_k \psi_{f,k}^\dagger \psi_{f,k} + (V_S - V_D) \frac{\psi_f^\dagger(0) - \psi_f(0)}{\sqrt{2}} \chi_1 \\ &\quad + i(V_S + V_D) \frac{\psi_f^\dagger(0) + \psi_f(0)}{\sqrt{2}} \chi_2 + i\epsilon_R \chi_1 \chi_2, \end{aligned} \quad (15)$$

Straightforwardly, at the quantum critical point where $\epsilon_R = 0$ and $V_S = V_D$, one impurity Majorana γ_1 becomes isolated, thus leading to the $\ln\sqrt{2}$ residual entropy.

In the rest of the paper, we focus on the symmetric point $V_S = V_D \equiv V_R$, and couple this system to the right end of the superconducting nanowire as a stabilizer.

IV. CONDUCTANCE IN THE DETECTOR: THREE CASES

With the system introduced, we calculate the conductance G_L through the left quantum dot (the detector) in different scenarios.

A. No Stabilizer

For the simplest scenario, without the presence of any stabilizer, γ_2 couples only to its partner γ_1 . This case has been studied previously [32]: the non-trivial zero-temperature conductance $e^2/2h$ abruptly becomes the trivial one e^2/h upon *any* non-zero ϵ_M . From the RG perspective, this means that ϵ_M is relevant and thus when temperature decreases ϵ_M effectively *increases*.

B. Frustration-Induced Degeneracy in Right Dot

With the presence of the dissipative resonant level, the key final ingredient in our problem is the connection between the right dot and the topological wire. This is simply tunneling, as for the left dot Eq. (3); for detailed discussions of tunneling between tMZM and those arising from Klein factors in bosonization see, e.g., Refs. [55–57]. Generically, γ_2 couples to both χ_1 and χ_2 , yielding the Hamiltonian

$$H_{\text{sys.-dis.}} = +it_{R1} \gamma_2 \chi_1 + it_{R2} \gamma_2 \chi_2 \quad (16)$$

with arbitrary couplings t_{R1} and t_{R2} .

The full Hamiltonian for our problem, $H = H_{\text{sys.}} + H_{\text{detect.}} + H_{\text{dissip.}} + H_{\text{sys.-det.}} + H_{\text{sys.-dis.}}$, is quadratic and so can be solved through the equation of motion method. We calculate the conductance of the left quantum dot that probes the γ_1 tMZM. With symmetric coupling, its equilibrium conductance is related to the dot spectral function by

$$G_L = -\Gamma_L \frac{e^2}{h} \int \frac{d\omega}{2\pi} \text{Im} \left\{ G^R(d_L, d_L^\dagger)(\omega) \right\} \partial_\omega n_F(\omega), \quad (17)$$

where $G^R(d_L, d_L^\dagger)(\omega)$ is the Fourier transform of the retarded Green function $-i\theta(t)\langle\{d_L(0), d_L^\dagger(t)\}\rangle$, $n_F(\omega)$ is the Fermi distribution function, and $\Gamma_L = \pi\rho_0 V_L^2$ is the level broadening.

The retarded Green function of the left dot from the equation of motion method [58] is

$$G^R(d_L, d_L^\dagger)(\omega) = \frac{1}{\omega + i\Gamma_L - \epsilon_L - \Sigma(\omega)}, \quad (18)$$

where the self-energy $\Sigma(\omega)$ incorporates the effects of the coupling between (i) the left dot and γ_1 , (ii) γ_1 and γ_2 Eq. (1), and (iii) γ_2 and the right dot Eq. (16)). With the presence of the dissipative stabilizer, the self energy is

$$\begin{aligned} \Sigma(\omega)^{-1} &= \frac{\omega}{t_L^2} - \frac{1}{\omega + \epsilon_L + i\Gamma_L} \\ &- \frac{\epsilon_M^2}{t_L^2} \left(\omega - \frac{t_{R1}^2}{\omega + \epsilon_R + i\eta} - \frac{t_{R1}^2}{\omega - \epsilon_R + i\eta} \right)^{-1} \\ &- \frac{\epsilon_M^2}{t_L^2} \left(\omega - \frac{t_{R2}^2}{\omega + \epsilon_R + i\Gamma_R} - \frac{t_{R2}^2}{\omega - \epsilon_R + i\Gamma_R} \right)^{-1}, \end{aligned} \quad (19)$$

where η is a positive infinitesimal and $\Gamma_R = \pi\rho_0 V_R^2$ is the level broadening of the right dot in the absence of dissipation.

With Eqs. (18) and (19), the conductance through the left dot when $\epsilon_R = 0$ is

$$G_L = \frac{1}{2} \frac{e^2}{h}, \quad (20)$$

independent of the values of any parameters (such as t_{R2} or ϵ_M). This striking independence implies, for instance, that fine tuning of the coupling between γ_2 and the right dot is *not* needed, a significant experimental simplification. This result holds only within the validity of our model, of course: one should have $\epsilon_M \ll \Delta$ in order to have the tMZM pair (Δ is

the superconducting gap in the proximitized nanowire) and $\epsilon_M \ll \Gamma_R$ in order to have a fMZM from frustration.

The conductance Eq. (20) is one of our main results. It indicates that the introduction of the $R=R_Q$ dissipative quantum dot stabilizes γ_1 .

We emphasize that the stabilization of γ_1 refers to the fact that at zero temperature ϵ_M always effectively vanishes. This is true even if ϵ_M is significant initially, such as in a system with a short nanowire. This complete stabilization is uniquely guaranteed by the presence of the fMZM: it couples with γ_2 into a singlet, thus preventing the inter-tMZM coupling. We further illustrate this point in Sec. IV D below through analysis with the g-theorem.

Fine-tuning of the energy level of the quantum dot is required only for the right-hand dot, $\epsilon_R = 0$. We do not need a fine-tuned left dot since ϵ_L is irrelevant at the nontrivial fixed point: at this point, γ_1 and $(d_L^\dagger + d_L)/\sqrt{2}$ form a singlet, thus strongly suppressing the hybridization between $(d_L^\dagger + d_L)/\sqrt{2}$ and $(d_L^\dagger - d_L)/i\sqrt{2}$. Experimentally, the irrelevance of ϵ_L is a signature of the tMZM: instead of the usual Lorentzian shape from the resonant level model, the zero temperature conductance of the left-hand dot is expected to be *flat* as a function of ϵ_L . For non-zero temperature, the conductance will be constant as long as $\epsilon_L(T) < \Gamma_L(T)$, both of which may vary with temperature because of renormalization effects.

C. Dissipation-Free Right Dot

To highlight the role of dissipation, we now consider what happens if there is no dissipation in the right-hand leads, $r=0$. Thus the full-transmission fixed point Hamiltonian Eq. (15) is replaced by a second copy of the resonant level Hamiltonian Eq. (2). Since the Hamiltonian remains quadratic, we again use the equation of motion method to find the retarded Green function of the left dot; the explicit form of the self-energy now becomes

$$\begin{aligned} \Sigma(\omega)^{-1} &= \frac{\omega}{t_L^2} - \frac{1}{\omega + \epsilon_L + i\Gamma_L} \\ &- \frac{\epsilon_M^2}{t_L^2} \left(\omega - \frac{t_R^2}{\omega + \epsilon_R + i\Gamma_R} - \frac{t_R^2}{\omega - \epsilon_R + i\Gamma_R} \right)^{-1}. \end{aligned} \quad (21)$$

In the absence of dissipation, the two MZMs on the right dot become equivalent, allowing us to freely choose γ_2 to couple to any linear combination of them with the coupling strength t_R . The remaining MZM will be hybridized by the leads.

The conductance of the left quantum dot in this case is

$$G_L = \frac{e^2}{h} \frac{2t_L^2 t_R^2 + \epsilon_M^2 \Gamma_L \Gamma_R}{4t_L^2 t_R^2 + \epsilon_M^2 \Gamma_L \Gamma_R}, \quad (22)$$

where $\Gamma_R = \pi\rho_0 V_R^2$ is the broadening of the right resonant level. Eq. (22) displays an interesting feature: the equilibrium zero temperature conductance varies *continuously* between the trivial (e^2/h) and the non-trivial ($e^2/2h$) values, depending on the details of the system. This crossover originates from the competition between the dot-MZM couplings and the hybridization of the quantum dots by the leads.

	$t_R = 0$	$t_R \neq 0$ and $R = 0$	$t_R \neq 0$ and $R = R_Q$
g_{trivial}	1	1	$\sqrt{2}$
$g_{\text{nontrivial}}$	$\sqrt{2}$	1	1
$G_L/(e^2/h)$	1	$\frac{2t_L^2 t_R^2 + \epsilon_M^2 \Gamma_L \Gamma_R}{4t_L^2 t_R^2 + \epsilon_M^2 \Gamma_L \Gamma_R}$	1/2

TABLE I. System characteristics at different fixed points. Here, g_{trivial} and $g_{\text{nontrivial}}$ are the degeneracies of the trivial and nontrivial fixed points, respectively, and G_L is the zero temperature conductance through the left dot. For simplicity we have used $t_R = 0$ to label the decoupling of the right dot.

Eq. (22) implies that ϵ_M is effectively controllable through fine-tuning $t_{L,R}$ and $\Gamma_{L,R}$. Indeed, this result agrees with previous investigations of quantum dots coupled to proximitized nanowires in which non-local effects produced by the two tMZM (which are related directly to the value of ϵ_M) are tunable through fine-tuning of the dot level [2, 28–30]. We stress that in these systems the effective inter-tMZM overlap is only reduced. In strong contrast, with the fMZM induced by dissipation in our system, this overlap is driven by interactions to *zero*.

D. Explanation with g-Theorem

To summarize briefly thus far, we have shown that the conductance through the MZM-coupled left quantum dot is strongly influenced by the nature of the system on the right. (i) In the absence of a right-hand system, the two MZMs γ_1 and γ_2 couple into a trivial state for which $G_L/(e^2/h) = 1$. (ii) When the right-hand system is present but without dissipation, the conductance through the left dot is between the trivial and nontrivial values, depending on the details of the system. (iii) Finally, the nontrivial state is stabilized when the right-hand system is dissipative with $R = R_Q$, leading to the zero-temperature conductance $G_L/(e^2/h) = 1/2$.

Through the g-theorem, we now provide a simple way to understand these results. As the counterpart of the famous c-theorem of two-dimensional conformal field theory [59, 60], the g-theorem treats boundary phase transitions and relates the stability of the fixed points to the impurity or boundary entropy. Specifically, if the bulk parameters remain invariant during the RG flows, the flow will bring the system toward the fixed point with a smaller impurity entropy [61, 62]. We have calculated the ground state degeneracy of our system at the two fixed points in the three scenarios above. The results are compiled in Table I, and we now discuss each scenario in turn.

(i) If the right-hand system is absent ($t_R = 0$) and $\epsilon_M \neq 0$, the trivial fixed point is non-degenerate: the two tMZMs γ_1 and γ_2 form into a singlet and the left quantum dot is completely hybridized with the leads. In contrast, the nontrivial fixed point has a decoupled tMZM, namely γ_2 , yielding a ground state degeneracy $\sqrt{2}$. The g-theorem then implies, in agreement with the conductance calculation above, that the nontrivial fixed point is unstable. Alternatively, we notice that

the leading operator at the nontrivial fixed point is the hybridization between the leads and $(d_L^\dagger + d_L)/\sqrt{2}$, which has the scaling dimension 1/2. Consequently, the hybridization operator is relevant and sabotages the nontrivial fixed point.

(ii) If the right-hand system is a dissipationless quantum dot, the ground states of both the trivial and nontrivial fixed points are non-degenerate. Consequently, the operator that connects these two fixed points is marginal, leading to a crossover between the trivial and nontrivial fixed points. This crossover is reflected in the intermediate value of the conductance, Eq. (22). From an RG point of view, because the parity of the superconducting island is conserved, tunneling happens simultaneously in the left and right quantum dots (see Appendix for details). Thus the scaling dimension of the hybridization doubles compared to case (i), rendering it marginal.

(iii) Finally, when the right quantum dot is dissipative, at the nontrivial fixed point the isolated fMZM χ_2 couples to γ_2 in a singlet, thus leading to a non-degenerate ground state. In contrast, at the trivial fixed point, χ_2 remains isolated, yielding degeneracy $\sqrt{2}$. Consequently, the g-theorem predicts that the RG flow brings the system toward the *nontrivial* fixed point. Alternatively, the lead-dot hybridization is suppressed by the dissipation and so has a larger scaling dimension than in case (ii). The hybridization thus becomes irrelevant (for any $R \neq 0$) and the Majorana feature is protected. This protection uniquely exists in a dissipative or an interacting system where a non-trivial (i.e., the Majorana-like) residual entropy has been added to the system through the frustration between two competing dissipative leads.

V. FULL COUNTING STATISTICS

In the previous section, we investigate the zero-temperature linear-response conductance through the left quantum dot. Our calculation indicates that the effective ϵ_M exactly vanishes when γ_2 couples to a dissipative quantum dot, thus completely stabilizing γ_1 from the inter-tMZM coupling. In this section, we instead investigate the *non-equilibrium* current and shot noise of the model at different fixed points with full counting statistics [63–65]. Since analysis in previous sections indicates that t_{R2} is RG irrelevant in the presence of finite t_{R1} , we take $t_{R2} = 0$ for simplicity.

A. Full Counting Statistic in the Majorana-Fermion-Coupled Resonant Level Model

In full counting statistics, the current and noise are calculated through [63]

$$I = \frac{e \langle \delta q \rangle}{\tau}, \quad \text{and} \quad S = \frac{2e^2 \langle \delta^2 q \rangle}{\tau}, \quad (23)$$

where the moments

$$\langle \delta^n q \rangle = (-i)^n \frac{\partial^n}{\partial \lambda^n} \ln \chi(\lambda) \Big|_{\lambda=0} \quad (24)$$

characterize the charge correlations. In Eq. (24), the generating function $\chi(\lambda) = \sum_q e^{iq\lambda} P_q(\tau)$ includes tunneling events to all orders ($q \in \mathbb{Z}^{\geq}$ is a non-negative integer), where λ is the measuring field and $P_q(\tau)$ is the probability that charge qe tunnels through the barrier(s) during the measuring time τ . Practically, in 1D systems $\ln \chi(\lambda) = -i\tau U(\lambda, -\lambda)$ where $U(\lambda, -\lambda)$ is the adiabatic potential.

For the left quantum dot of our system (the detector), the adiabatic potential of the resonant level model is

$$\begin{aligned} & \frac{\partial}{\partial \lambda_-} U(\lambda_-, \lambda_+) \\ &= \frac{V_L^2}{2} \int d\omega \left[e^{-i(\lambda_- - \lambda_+)/2} G^<(d_L, d_L^\dagger) g_{L\alpha}^{+-} \right. \\ & \quad \left. - e^{i(\lambda_- - \lambda_+)/2} g_{L\alpha}^{-+} G^>(d_L, d_L^\dagger) \right], \end{aligned} \quad (25)$$

where $G^>(d, d^\dagger)$ [$G^<(d, d^\dagger)$] is the full greater (lesser) impurity Green function and $g_{L\alpha}$ is the bare Green function for the source or drain lead ($\alpha = S$ or D). The four components of the bare lead Green function are given by [64, 65]

$$\begin{aligned} g_{L\alpha}^{--}(\omega) &= g_{\alpha}^{++}(\omega) = i2\pi\rho_0(n_\alpha - 1/2), \\ g_{L\alpha}^{-+}(\omega) &= i2\pi\rho_0 n_\alpha, \\ g_{L\alpha}^{+-}(\omega) &= -i2\pi\rho_0(1 - n_\alpha), \end{aligned} \quad (26)$$

where $n_{S,D} = n_F(\epsilon \pm V/2)$ is the distribution function of the leads and $V > 0$ is the bias applied between source and drain. At zero temperature, these distribution functions simplify to $n_S = \Theta(-\epsilon - V/2)$ and $n_D = \Theta(-\epsilon + V/2)$.

To calculate the full Green functions $G^<$ and $G^>$, we divide the Hamiltonian into two parts $H = H_0 + \delta H$, where $H_0 =$

$H_{\text{sys.}} + H_{\text{detect.}} + H_{\text{dissip.}} + H_{\text{sys.-dis.}}$ contains the non-equilibrium resonant level model (the detector) plus the other parts of the system, while $\delta H = H_{\text{sys.-det}}$ connects these two parts.

When $\delta H = 0$ ($t_L = 0$), these two parts are disconnected, and we can calculate the Green functions of them separately. The non-equilibrium Green function matrix $G_0(d_L, d_L^\dagger)$ of the resonant level Hamiltonian $H_{\text{detect.}}$ is known [64],

$$\begin{aligned} G_0(d_L, d_L^\dagger)(\omega) &= \begin{bmatrix} G_0^R(d_L, d_L^\dagger)(\omega) & G_0^<(d_L, d_L^\dagger)(\omega) \\ G_0^>(d_L, d_L^\dagger)(\omega) & G_0^A(d_L, d_L^\dagger)(\omega) \end{bmatrix} \\ &= \frac{1}{\omega^2 + \Gamma_L^2} \begin{pmatrix} \omega - i\Gamma_L & ie^{i\lambda}\Gamma_L \\ -i\Gamma_L & -\omega - i\Gamma_L \end{pmatrix}, \end{aligned} \quad (27)$$

with the four entries referring to the retarded, lesser, greater and advanced Green functions, respectively (from top to bottom, left to right). Note that the measuring field λ appears. The remaining parts of the system ($H_{\text{sys.}} + H_{\text{dissip.}} + H_{\text{sys.-dis.}}$), on the other hand, remain in equilibrium when $t_L = 0$. We thus obtain the equilibrium retarded Green function of γ_1 ,

$$G_0^R(\gamma_1, \gamma_1)(\omega) = \frac{\omega^2 - t_R^2}{\omega(\omega^2 - t_R^2 - \epsilon_M^2)}. \quad (28)$$

With δH , we calculate the full lesser Green function through the Dyson equation [64–66]

$$\begin{aligned} G^< &= G^R \Sigma^< G^A \\ &+ (1 + G^R \Sigma^R) G_0^< (1 + \Sigma^A G^A). \end{aligned} \quad (29)$$

After including all possible processes, Eq. (29) becomes

$$\begin{aligned} G^<(d_L, d_L^\dagger)(\omega) &= G_0^<(d_L, d_L^\dagger)(\omega) + G^R(d_L, \gamma_1) \Sigma_{\gamma_1, d_L}^R G_0^<(d_L, d_L^\dagger) \Sigma_{d_L^\dagger, \gamma_1}^A G^A(\gamma_1, d_L^\dagger)(\omega) \\ &+ G^R(d_L, \gamma_1) \Sigma_{\gamma_1, d_L^\dagger}^R G_0^<(d_L^\dagger, d_L) \Sigma_{d_L, \gamma_1}^A G^A(\gamma_1, d_L^\dagger)(\omega) \\ &+ G^R(d_L, \gamma_1)(\omega) \Sigma_{\gamma_1, d_L}^R G_0^<(d_L, d_L^\dagger) + G_0^<(d_L, d_L^\dagger) \Sigma_{d_L^\dagger, \gamma_1}^A G^A(\gamma_1, d_L^\dagger)(\omega), \end{aligned} \quad (30)$$

where the interaction terms $\Sigma_{d_L^\dagger, \gamma_1}^A = \Sigma_{\gamma_1, d_L}^R = -\Sigma_{\gamma_1, d_L^\dagger}^R = -\Sigma_{d_L, \gamma_1}^A = t_L$, and the impurity function $G_0^<(d_L^\dagger, d_L)$ equals

$$G_0^<(d_L^\dagger, d_L)(\omega) = \frac{-i\Gamma_L e^{-i\lambda}}{\omega^2 + \Gamma_L^2 e^{-i\lambda}}. \quad (31)$$

Eq.(30) contains two additional Green functions, $G^R(d_L, \gamma_1)(\omega)$ and $G^A(\gamma_1, d_L^\dagger)(\omega)$, that can also be

found from Dyson equations:

$$\begin{aligned} G^R(d_L, \gamma_1)(\omega) &= 0 + G_0^R(d_L, d_L^\dagger)(\omega) \Sigma_{d_L^\dagger, \gamma_1} G^R(\gamma_1, \gamma_1)(\omega), \\ G^R(\gamma_1, \gamma_1)(\omega) &= G_0^R(\gamma_1, \gamma_1)(\omega) \\ &+ G_0^R(\gamma_1, \gamma_1)(\omega) \Sigma_{\gamma_1, d_L} G^R(d_L, \gamma_1)(\omega) \\ &+ G_0^R(\gamma_1, \gamma_1)(\omega) \Sigma_{\gamma_1, d_L^\dagger} G^R(d_L^\dagger, \gamma_1)(\omega), \\ G^R(d_L^\dagger, \gamma_1)(\omega) &= 0 + G_0^R(d_L^\dagger, d_L)(\omega) \Sigma_{d_L, \gamma_1} G^R(\gamma_1, \gamma_1)(\omega). \end{aligned} \quad (32)$$

Eqs.(27)-(32) yield the lesser Green function required in Eq.(25). Following analogous steps, we also obtain the greater Green function. Combining these with the bare lead Green functions Eq.(26), we obtain the adiabatic potential and the generating function from Eq.(25). This finally allows

evaluation of the the current and noise, Eq. (23) [67].

Below we present expressions for the non-equilibrium current and noise in different cases corresponding to different fixed points. Though from the calculation sketched here, we have the full nonlinear dependence on the bias V , for simplicity we expand the expressions to leading order in V [67], following the assumption that the bias V is smaller than all other relevant energy scales.

B. Non-Interacting tMZMs ($\epsilon_M = 0$)

We begin with the simple case $\epsilon_M = 0$. In this case, γ_1 is stable since it totally decouples from its partner γ_2 , and the result thus is independent of the presence of a stabilizer. The current calculated from the adiabatic potential in this case is

$$I(V) = \frac{e^2}{h} \left[\frac{V}{2} - \left(\frac{1}{\Gamma_L^2} - \frac{\Gamma_L^2}{4t_L^4} \right) \frac{e^2}{24} V^3 + \mathcal{O}(V^4) \right], \quad (33)$$

where $\mathcal{O}(V^4)$ indicates the neglected higher-order terms. Note that in agreement with Eq. (22) the linear-response conductance from this calculation is $e^2/2h$. As discussed above and in [32], this comes about because one of the left dot's Majorana degrees of freedom is fully coupled to the tMZM while the other fully hybridizes with the lead to form a transparent half-channel.

Interestingly, the cubic term [$\mathcal{O}(V^3)$] in (33) displays a competition between two processes: (i) backscattering in the transparent half-channel which reduces the current and (ii) hybridization of the left leads with $(d_L + d_L^\dagger)/\sqrt{2}$, pulling it away from the tMZM and thereby enhancing the current. More specifically, when $\Gamma^2 > 2t_L^2$ the hybridization is stronger so that the $\mathcal{O}(V^3)$ current increases with an increasing bias and vice versa. Note that the presence of this competition requires two Majorana channels in opposite limits—one completely healed and the other totally disconnected. To the best of our knowledge, such a situation exists only in systems that are topological.

Turning to the fluctuations of the current, we find that the zero-temperature shot noise to leading order is

$$S = 2 \frac{e^3}{h} \left[\frac{V}{4} + \left(-\frac{1}{\Gamma_L^2} - \frac{\Gamma_L^2}{4t_L^4} + \frac{1}{t_L^2} \right) \frac{e^2}{48} V^3 + \mathcal{O}(V^4) \right], \quad (34)$$

with the leading term proportional to bias. This linear term is a signal that the transmission is *not* perfect: for a system with perfect transmission, the leading term should instead be $\propto V^3$ [see Eq. (36) for an example when $\epsilon_M \neq 0$].

The competing effects seen in the nonlinear current also appear here. Indeed, noise to the next-leading order [i.e., $\mathcal{O}(V^3)$] reaches it maximum when two competing processes equal (i.e., $\Gamma^2 = 2t_L^2$). This point, with half transmission probability, is known to have the largest shot noise [68].

Near equilibrium, the Fano factor, $F \equiv S/2eI$, becomes $1/2$, implying that the current is carried by quasi-particles with effective charge $e^* = e/2$ at zero temperature. As in

the charge 2CK case discussed in [69], here the $e^* = e/2$ fractional charge property originates from the fact that one of the Majorana channels in the leads completely decouples (Fig. 2).

C. Interacting tMZMs without Stabilization

Now we add back the interaction between two tMZMs ($\epsilon_M \neq 0$), but do not include the right-hand quantum dot ($t_R = 0$) as the stabilizer.

The nonlinear current calculated with full counting statistics now becomes

$$I(V) = \frac{e^2}{h} \left[V - \frac{1 + 2t_L^2/\epsilon_M^2 + 2t_L^4/\epsilon_M^4}{12\Gamma_L^2} e^2 V^3 + \mathcal{O}(V^4) \right], \quad (35)$$

with the trivial equilibrium conductance e^2/h , in agreement with Ref. [32]. In contrast to Eq. (33), there is no sign of competing effects in the nonlinear term. Indeed, at a perfectly conducting fixed point, non-equilibrium effects necessarily reduce the conductance, so the sign of the V^3 term is fixed.

The shot noise now becomes

$$S = 2 \frac{e^3}{h} \left[\left(\frac{t_L^4}{\epsilon_M^4} + 1 \right) \frac{e^2}{12\Gamma_L^2} V^3 + \mathcal{O}(V^4) \right], \quad (36)$$

with the leading term $\propto V^3$. Eq. (36) contains both backscattering-induced noise and noise generated by the coupling between γ_1 and $i(-d_L + d_L^\dagger)$. Notice the factor ϵ_M^4 in the denominator here as well as in the nonlinear current Eq. (35). The high power indicates that ϵ_M is RG relevant and drives the system to a different fixed point when it is non-zero.

Since the linear term in the shot noise vanishes, here the Fano factor can be defined as the ratio between shot noise and twice the value of the “backscattering current” as in the charge 2CK model [69]. Using the V^3 terms in both the current and the shot noise, Eqs. (35) and (36), we see that the Fano factor depends on the ratio t_L/ϵ_M . We prefer not to discuss an effective charge of the quasi-particle in this case since the inelastic contributions to the nonlinear terms complicate the interpretation [70]. The variation of the Fano factor indicates that at the quantum dot, an electron either backscatters or tunnels into the superconducting island.

D. Interacting tMZMs Stabilized by Frustration

Comparison of the results in these two cases (Sections VB and VC) supports our analysis that the coupling ϵ_M between the two tMZMs is relevant, leading to the destruction of the Majorana signature in the detector. In this section we add the frustration-induced Majorana fermion χ_1 and show that it stabilizes the probed tMZM γ_1 .

In this case, the model in Section IV B yields the current

$$I(V) = \frac{e^2}{h} \left[\frac{V}{2} + \left(\frac{\epsilon_M^4 \Gamma_L^2}{t_L^4 t_R^4} + \frac{2\epsilon_M^2 \Gamma_L^2}{t_L^4 t_R^2} + \frac{\Gamma_L^2}{t_L^4} - \frac{4}{\Gamma_L^2} \right) \frac{e^2}{96} V^3 + \mathcal{O}(V^4) \right], \quad (37)$$

with the expected linear-response conductance $e^2/2h$, Eq. (20). Note further that the full $I(V)$ reduces to Eq. (33) when $\epsilon_M = 0$. The fact that ϵ_M is in the numerator in the nonlinear term shows that it is RG irrelevant. This is, then, verification of our analysis that the presence of χ_1 stabilizes γ_1 against the inter-tMZM coupling ϵ_M .

The shot noise now becomes

$$S = 2 \frac{e^2}{h} \left[\frac{V}{4} + \left(-\frac{1}{4\Gamma^2} - \frac{\Gamma^2}{16t_L^4} + \frac{1}{4t_L^2} - \frac{\epsilon_M^4 \Gamma^2}{16t_L^4 t_R^4} - \frac{\epsilon_M^2 \Gamma^2}{8t_L^4 t_R^2} + \frac{\epsilon_M^2}{4t_L^2 t_R^2} \right) \frac{e^2}{12} V^3 + \mathcal{O}(V^4) \right]. \quad (38)$$

In the V^3 term, the inter-tMZM coupling ϵ_M again appears only in the numerator, showing its RG irrelevance. This allows a smooth $\epsilon_M \rightarrow 0$ limit yielding, indeed, Eq. (34). The shot noise here does have a fixed linear term. As in the $\epsilon_M = 0$ case, from the Fano factor we deduce tunneling of quasiparticles with effective charge $e^* = e/2$.

These results for both the nonlinear transport $I(V)$ and the shot noise, then, support our equilibrium result (Section IV) that χ_1 stabilizes the tMZM γ_1 against its coupling to γ_2 .

VI. SUMMARY

The effect that we elucidate here arises in essence from combining a Majorana degree of freedom due to topology with a Majorana produced by fine-tuned quantum frustration (i.e. interactions). This is a highly unusual situation: we connect a topological system with one that is not topological and find no unusual feature at the boundary (and in particular no MZM).

We arrive at this result by, first, calculating the conductance through a detector quantum dot and, second, supporting the calculation through RG arguments and the g-theorem. The combination of the two types of MZM originates from the preference of the system for a non-degenerate ground state, arrived at by coupling the topological Majorana γ_2 and the quantum dot Majorana fermion χ_1 into a singlet. Our conclusions are further supported by a fully non-equilibrium calculation in which the nonlinear current and shot noise reveal signatures of the RG relevant and irrelevant processes.

Perhaps the most interesting implication of our results for future work is that the long-ignored frustration generated Majorana fermion is in principle detectable. Indeed, it could be potentially beneficial for quantum computation.

Acknowledgements— We thank Ruixing Zhang for fruitful discussions. The work at Duke was supported by the U.S. DOE Office of Science, Division of Materials Sciences and Engineering, under Grant No. DE-SC0005237.

Appendix A: Parity Conservation Induced Joint Tunneling

In this appendix, we briefly explain a striking feature caused by the presence of tMZMs: parity conservation induced *joint tunneling* at both sides of the superconducting nanowire.

We consider the system near the strong coupling fixed point, where the impurity part consists of two tMZMs ($\gamma_{1,2}$) and two un-hybridized impurity Majorana fermions ($d_{L,R}^\dagger + d_{L,R}$)/ $\sqrt{2}$. For the nontrivial case ($\epsilon_M = 0$), the quantum dot MZMs ($d_{L,R}^\dagger + d_{L,R}$)/ $\sqrt{2}$ form into singlets with their corresponding tMZMs $\gamma_{1,2}$. For simplicity, we label this state $|0\rangle_L \otimes |0\rangle_R$. We further label the excited state on each side as $|1\rangle_{L,R}$, respectively.

Now we add the weak inter-tMZM coupling ϵ_M , which alters the system ground state. In this case we find the ground state of the impurity system with the Hamiltonian

$$H'_{\text{impurity}} = it_L(d_L^\dagger + d_L)\gamma_1 + it_R(d_R^\dagger + d_R)\gamma_2 + i\epsilon_M\gamma_1\gamma_2 \quad (A1)$$

through exact diagonalization. Without loss of generality, we take $t_L = t_R = t$ for simplification. The ground state has energy $\sqrt{2}t - \sqrt{\epsilon_M^2 + 8t^2}/2$ with eigenvector

$$\frac{i(-2\sqrt{2}u + \sqrt{1 + 8u^2})|0\rangle_L \otimes |0\rangle_R + |1\rangle_L \otimes |1\rangle_R}{\sqrt{1 + (-2\sqrt{2}u + \sqrt{1 + 8u^2})^2}}, \quad (A2)$$

where $u \equiv t/\epsilon_M$. Eq. (A2) correctly reduces to $|0\rangle_L \otimes |0\rangle_R$ in the limit $\epsilon_M \rightarrow 0$.

Eq. (A2) indicates that the system ground state involves dot states with only even parity $|0\rangle_L \otimes |0\rangle_R$ and $|1\rangle_L \otimes |1\rangle_R$. Physically, this originates from the fact that the inter-tMZM coupling operator $\epsilon_M\gamma_1\gamma_2$ changes the parity of the impurity states at *both* sides. Consequently, if we now turn on weak tunneling to the corresponding leads in both quantum dots (the resonant level model), the system allows only tunneling events that occur *simultaneously* at both sides, thus doubling the scaling dimension of the leading-order terms.

-
- [1] S. Das Sarma, Michael Freedman, and C. Nayak, “Majorana zero modes and topological quantum computation,” *npj Q. Inf.* **1**, 15001 (2015).
 [2] R. Aguado, “Majorana quasiparticles in condensed matter,” *La Rivista del Nuovo Cimento* **40**, 523–593 (2017), arXiv: 1711.00011.
 [3] R. M. Lutchyn, E. P. A. M. Bakkers, L. P. Kouwenhoven, P. Krogstrup, C. M. Marcus, and Y. Oreg, “Majorana zero

modes in superconductor-semiconductor heterostructures,” *Nat. Rev. Mat.* **3**, 52–68 (2018).

- [4] T. D. Stanescu, *Introduction to Topological Quantum Matter and Quantum Computation* (CRC Press, New York, 2017).
 [5] I. Affleck, A. W. W. Ludwig, H.-B. Pang, and D. L. Cox, “Relevance of anisotropy in the multichannel Kondo effect: Comparison of conformal field theory and numerical renormalization-group results,” *Phys. Rev. B* **45**, 7918–7935 (1992).

- [6] V. J. Emery and S. Kivelson, “Mapping of the two-channel kondo problem to a resonant-level model,” *Phys. Rev. B* **46**, 10812–10817 (1992).
- [7] E. Wong and I. Affleck, “Tunneling in quantum wires: A boundary conformal field theory approach,” *Nucl. Phys. B* **417**, 403–438 (1994).
- [8] I. Affleck, A. W. W. Ludwig, and B. A. Jones, “Conformal-field-theory approach to the two-impurity Kondo problem: Comparison with numerical renormalization-group results,” *Phys. Rev. B* **52**, 9528–9546 (1995).
- [9] A. O. Gogolin, A. A. Nersisyan, and A. M. Tsvelik, *Bosonization and Strongly Correlated Systems* (Cambridge University Press, Cambridge UK, 1998), Chapter 28.
- [10] Cristiano Nisoli, Roderich Moessner, and Peter Schiffer, “Colloquium: Artificial spin ice: Designing and imaging magnetic frustration,” *Rev. Mod. Phys.* **85**, 1473–1490 (2013).
- [11] Kenneth G. Wilson, “The renormalization group: Critical phenomena and the Kondo problem,” *Rev. Mod. Phys.* **47**, 773–840 (1975).
- [12] Ph. Nozières and A. Blandin, “Kondo effect in real metals,” *J. Phys. (France)* **41**, 193–211 (1980).
- [13] A. Zawadowski, “Kondo-like state in a simple model for metallic glasses,” *Phys. Rev. Lett.* **45**, 211–214 (1980).
- [14] The 2CK quantum critical point is only well defined with an infinite system, where the “partner” of the unpaired spin Majorana is pushed towards infinity.
- [15] C. Jayaprakash, H. R. Krishna-murthy, and J. W. Wilkins, “Two-impurity kondo problem,” *Phys. Rev. Lett.* **47**, 737–740 (1981).
- [16] H. T. Mebrahtu, I. V. Borzenets, H. Zheng, Yu. V. Bomze, A. I. Smirnov, S. Florens, H. U. Baranger, and G. Finkelstein, “Observation of Majorana quantum critical behavior in a resonant level coupled to a dissipative environment,” *Nat. Phys.* **9**, 732–737 (2013).
- [17] Huaixiu Zheng, Serge Florens, and H. U. Baranger, “Transport signatures of Majorana quantum criticality realized by dissipative resonant tunneling,” *Phys. Rev. B* **89**, 235135 (2014).
- [18] R. M. Potok, I. G. Rau, H. Shtrikman, Y. Oreg, and D. Goldhaber-Gordon, “Observation of the two-channel Kondo effect,” *Nature* **446**, 167–171 (2007).
- [19] H. T. Mebrahtu, I. V. Borzenets, Dong E. Liu, Huaixiu Zheng, Yu. V. Bomze, A. I. Smirnov, H. U. Baranger, and G. Finkelstein, “Quantum phase transition in a resonant level coupled to interacting leads,” *Nature* **488**, 61–64 (2012).
- [20] A. J. Keller, L. Peeters, C. P. Moca, I. Weymann, D. Mahalu, V. Umansky, G. Zarand, and D. Goldhaber-Gordon, “Universal Fermi liquid crossover and quantum criticality in a mesoscopic system,” *Nature* **526**, 237–240 (2015).
- [21] Z. Iftikhar, S. Jezouin, A. Anthore, U. Gennser, F. D. Parmentier, A. Cavanna, and F. Pierre, “Two-channel Kondo effect and renormalization flow with macroscopic quantum charge states,” *Nature* **526**, 233–236 (2015).
- [22] Z. Iftikhar, A. Anthore, A. K. Mitchell, F. D. Parmentier, U. Gennser, A. Ouerghi, A. Cavanna, C. Mora, P. Simon, and F. Pierre, “Tunable quantum criticality and super-ballistic transport in a “charge” Kondo circuit,” *Science*, 5592 (2018).
- [23] J. K. Pachos, *Introduction to Topological Quantum Computation* (Cambridge Univ. Press, Cambridge, UK, 2012).
- [24] Masatoshi Sato and Yoichi Ando, “Topological superconductors: a review,” *Rep. Prog. Phys.* **80**, 076501 (2017).
- [25] Hao-Hua Sun and Jin-Feng Jia, “Detection of Majorana zero mode in the vortex,” *npj Quant. Mater.* **2**, 1–9 (2017).
- [26] Arbel Haim and Yuval Oreg, “Time-reversal-invariant topological superconductivity in one and two dimensions,” *Phys. Rep.* **825**, 1–48 (2019).
- [27] Yukitoshi Motome and Joji Nasu, “Hunting Majorana fermions in Kitaev magnets,” *J. Phys. Soc. Jpn.* **89**, 012002 (2020).
- [28] M. T. Deng, S. Vaitiekėnas, E. B. Hansen, J. Danon, M. Leijnse, K. Flensberg, J. Nygård, P. Krogstrup, and C. M. Marcus, “Majorana bound state in a coupled quantum-dot hybrid-nanowire system,” *Science* **354**, 1557–1562 (2016).
- [29] Elsa Prada, Ramón Aguado, and Pablo San-Jose, “Measuring Majorana nonlocality and spin structure with a quantum dot,” *Phys. Rev. B* **96**, 085418 (2017).
- [30] David J. Clarke, “Experimentally accessible topological quality factor for wires with zero energy modes,” *Phys. Rev. B* **96**, 201109 (2017).
- [31] Fernando Domínguez, Jorge Cayao, Pablo San-Jose, Ramón Aguado, Alfredo Levy Yeyati, and Elsa Prada, “Zero-energy pinning from interactions in majorana nanowires,” *npj Quant. Mat.* **2**, 13 (2017).
- [32] Dong E. Liu and Harold U. Baranger, “Detecting a Majorana-fermion zero mode using a quantum dot,” *Phys. Rev. B* **84**, 201308 (2011).
- [33] Avraham Schiller and Selman Hershfield, “Exactly solvable nonequilibrium kondo problem,” *Phys. Rev. B* **51**, 12896–12899 (1995).
- [34] For clarification, by calling it “real”, we are emphasizing that this MZM contains only fermionic impurity operators. This fact is in strong contrast to that of the 2CK model, whose Majorana fermion consists of spin operators.
- [35] Dong E. Liu, Huaixiu Zheng, G. Finkelstein, and H. U. Baranger, “Tunable quantum phase transitions in a resonant level coupled to two dissipative baths,” *Phys. Rev. B* **89**, 085116 (2014).
- [36] G.-L. Ingold and Yu.V. Nazarov, “Charge tunneling rates in ultrasmall junctions,” in *Single Charge Tunneling: Coulomb Blockade Phenomena in Nanostructures*, edited by H. Grabert and M. H. Devoret (Plenum, New York, 1992) pp. 21–107, and arXiv:cond-mat/0508728.
- [37] Nazarov Yu.V. and Y. M. Blanter, *Quantum Transport : introduction to Nanoscience* (Cambridge University Press, Cambridge UK, 2009) p. 499, p. 499.
- [38] Uri Vool and Michel Devoret, “Introduction to quantum electromagnetic circuits,” *Intl. J. Circuit Theory App.* **45**, 897–934 (2017).
- [39] A. O. Caldeira and A. J. Leggett, “Influence of dissipation on quantum tunneling in macroscopic systems,” *Phys. Rev. Lett.* **46**, 211–214 (1981).
- [40] T. Giamarchi, *Quantum Physics in One Dimension* (Oxford University Press, Oxford UK, 2004).
- [41] P. W. Anderson, “A poor man’s derivation of scaling laws for the Kondo problem,” *J. Phys. C: Solid State Phys.* **3**, 2436 (1970).
- [42] J L Cardy, “One-dimensional models with $1/r^2$ interactions,” *Journal of Physics A: Mathematical and General* **14**, 1407 (1981).
- [43] C. L. Kane and M. P. A. Fisher, “Transmission through barriers and resonant tunneling in an interacting one-dimensional electron gas,” *Phys. Rev. B* **46**, 15233–15262 (1992).
- [44] S. Eggert and I. Affleck, “Magnetic impurities in half-integer-spin Heisenberg antiferromagnetic chains,” *Phys. Rev. B* **46**, 10866–10883 (1992).
- [45] K. A. Matveev and L. I. Glazman, “Coulomb blockade of tunneling into a quasi-one-dimensional wire,” *Phys. Rev. Lett.* **70**, 990–993 (1993).
- [46] Karsten Flensberg, “Capacitance and conductance of mesoscopic systems connected by quantum point contacts,” *Phys.*

- Rev. B* **48**, 11156–11166 (1993).
- [47] M. Sassetti and U. Weiss, “Transport of 1d interacting electrons through barriers and effective tunnelling density of states,” *EPL (Europhysics Letters)* **27**, 311 (1994).
- [48] I. Safi and H. Saleur, “One-channel conductor in an Ohmic environment: Mapping to a Tomonaga-Luttinger liquid and full counting statistics,” *Phys. Rev. Lett.* **93**, 126602 (2004).
- [49] K. Le Hur and Mei-Rong Li, “Unification of electromagnetic noise and Luttinger liquid via a quantum dot,” *Phys. Rev. B* **72**, 073305 (2005).
- [50] S. Jezouin, M. Albert, F. D. Parmentier, A. Anthore, U. Gennser, A. Cavanna, I. Safi, and F. Pierre, “Tomonaga-Luttinger physics in electronic quantum circuits,” *Nat. Commun.* **4**, 1802 (2013).
- [51] Gu Zhang, E. Novais, and H. U. Baranger, Non-Equilibrium Crossover near a Non-Fermi-Liquid Quantum Critical Point: Conductance of a Dissipative Quantum Dot, in preparation.
- [52] Anirvan M. Sengupta and Antoine Georges, “Emery-Kivelson solution of the two-channel Kondo problem,” *Phys. Rev. B* **49**, 10020–10022 (1994).
- [53] A. Schiller and S. Hershfield, “Toulouse limit for the nonequilibrium Kondo impurity: Currents, noise spectra, and magnetic properties,” *Phys. Rev. B* **58**, 14978 (1998).
- [54] Junwu Gan, “Solution of the two-impurity Kondo model: Critical point, Fermi-liquid phase, and crossover,” *Phys. Rev. B* **51**, 8287–8309 (1995).
- [55] B. Béri, “Majorana-Klein hybridization in topological superconductor junctions,” *Phys. Rev. Lett.* **110**, 216803 (2013).
- [56] Loïc Herviou, Karyn Le Hur, and Christophe Mora, “Many-terminal Majorana island: From topological to multichannel Kondo model,” *Phys. Rev. B* **94**, 235102 (2016).
- [57] D. Giuliano and I. Affleck, “Real fermion modes, impurity entropy, and nontrivial fixed points in the phase diagram of junctions of interacting quantum wires and topological superconductors,” *Nucl. Phys. B* **944**, 114645 (2019).
- [58] H. Bruus and K. Flensberg, *Many-Body Quantum Theory in Condensed Matter Physics* (Oxford University Press, New York, 2004).
- [59] A. B. Zomolodchikov, ““Irreversibility” of the flux of the renormalization group in a 2d field theory,” *JETP Lett* **43**, 730 (1986).
- [60] John L. Cardy, “Is there a c-theorem in four dimensions?” *Physics Letters B* **215**, 749 – 752 (1988).
- [61] Ian Affleck and Andreas W. W. Ludwig, “Universal noninteger “ground-state degeneracy” in critical quantum systems,” *Phys. Rev. Lett.* **67**, 161–164 (1991).
- [62] D. Friedan and A. Konechny, “Boundary Entropy of One-Dimensional Quantum Systems at Low Temperature,” *Phys. Rev. Lett.* **93**, 030402 (2004).
- [63] L. S. Levitov and M. Reznikov, “Counting statistics of tunneling current,” *Phys. Rev. B* **70**, 115305 (2004).
- [64] A. O. Gogolin and A. Komnik, “Towards full counting statistics for the Anderson impurity model,” *Phys. Rev. B* **73**, 195301 (2006).
- [65] A. Kamenev, *Field Theory of Non-Equilibrium Systems* (Cambridge University Press, 2011).
- [66] E. Sela and I. Affleck, “Nonequilibrium critical behavior for electron tunneling through quantum dots in an Aharonov-Bohm circuit,” *Phys. Rev. B* **79**, 125110 (2009).
- [67] We have included a Mathematica notebook as a supplementary material. In this notebook, we provide (i) complete expressions for and (ii) detailed derivation of the current and shot noise results of Sec. V.
- [68] Thomas Ihn, *Semiconductor Nanostructures* (Oxford Univ. Press, Oxford UK, 2010).
- [69] L. Aviad Landau, Eyal Cornfeld, and Eran Sela, “Charge fractionalization in the two-channel Kondo effect,” *Phys. Rev. Lett.* **120**, 186801 (2018).
- [70] Eran Sela, Yuval Oreg, Felix von Oppen, and Jens Koch, “Fractional shot noise in the Kondo regime,” *Phys. Rev. Lett.* **97**, 086601 (2006).